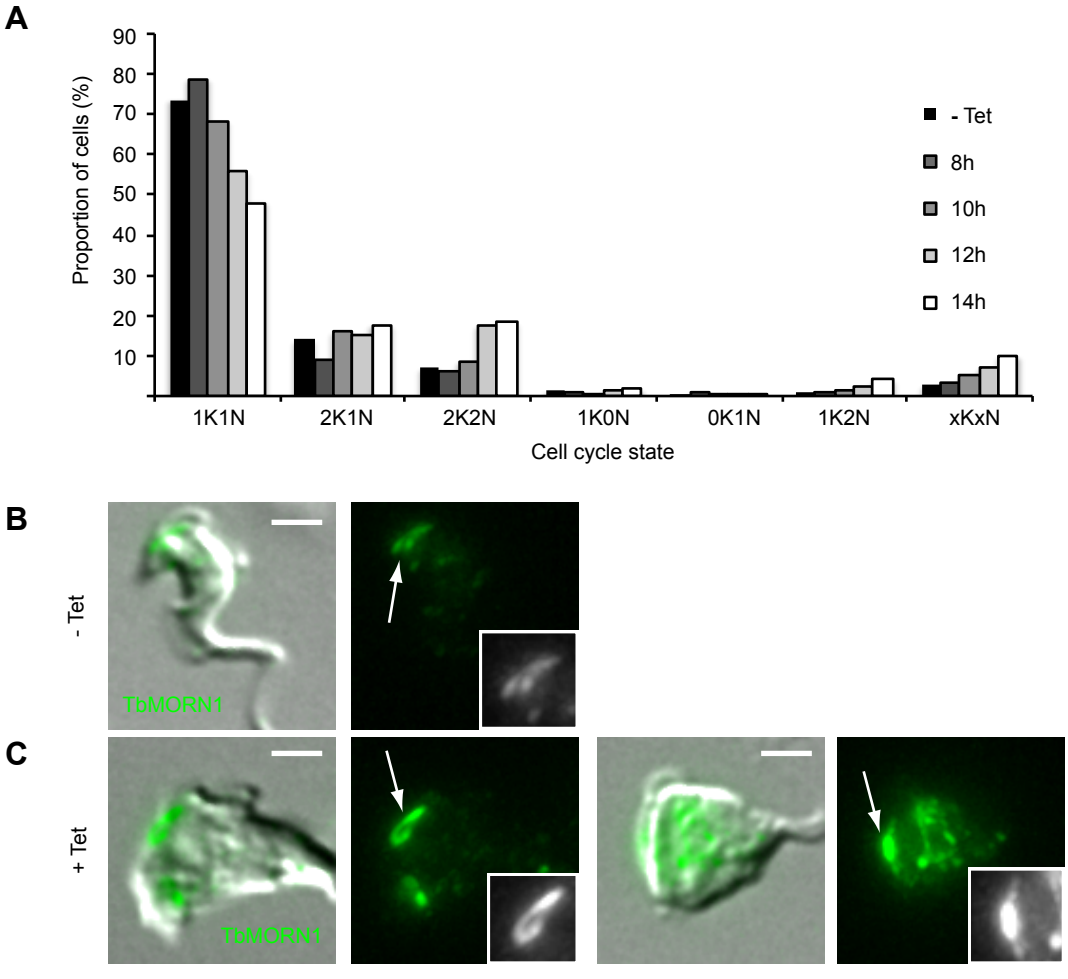

FIG. S1 Cell cycle analysis of TbMORN1-depleted cells and the impact of unplanned pre-permeabilisation (A) Depletion of TbMORN1 does not produce a strong effect on cell cycle state. TbMORN1 RNAi cells were fixed isothermally using glutaraldehyde, and DNA labeled using DAPI. Cell cycle state can be quantified from the relative numbers of kinetoplasts (K) and nuclei (N) in each cell. Uninduced (- Tet) cells were quantified as a control. TbMORN1-depleted cells were analyzed 8, 10, 12, 14 h post-induction. At the 12 h timepoint, there was a roughly twofold rise in the number of 2K2N cells. Data were collected from three independent experiments, and the number of cells in each cell cycle state expressed as a fraction of the total. N>250 cells for each time point. (B) Immunofluorescence labeling of a representative paraformaldehyde-fixed control cell with anti-TbMORN1 antibodies. The anti-TbMORN1-labeled structure (arrow) is enlarged in the greyscale inset. (C) Immunofluorescence labeling of paraformaldehyde-fixed cells with anti-TbMORN1 antibodies following depletion of TbMORN1 (14 h timepoint). The labeled structures (arrows) are enlarged in the greyscale insets. Note that the intensity of the signal is greater in both examples than that seen in section B despite using the same exposure time. Scale bars, 2 μm.

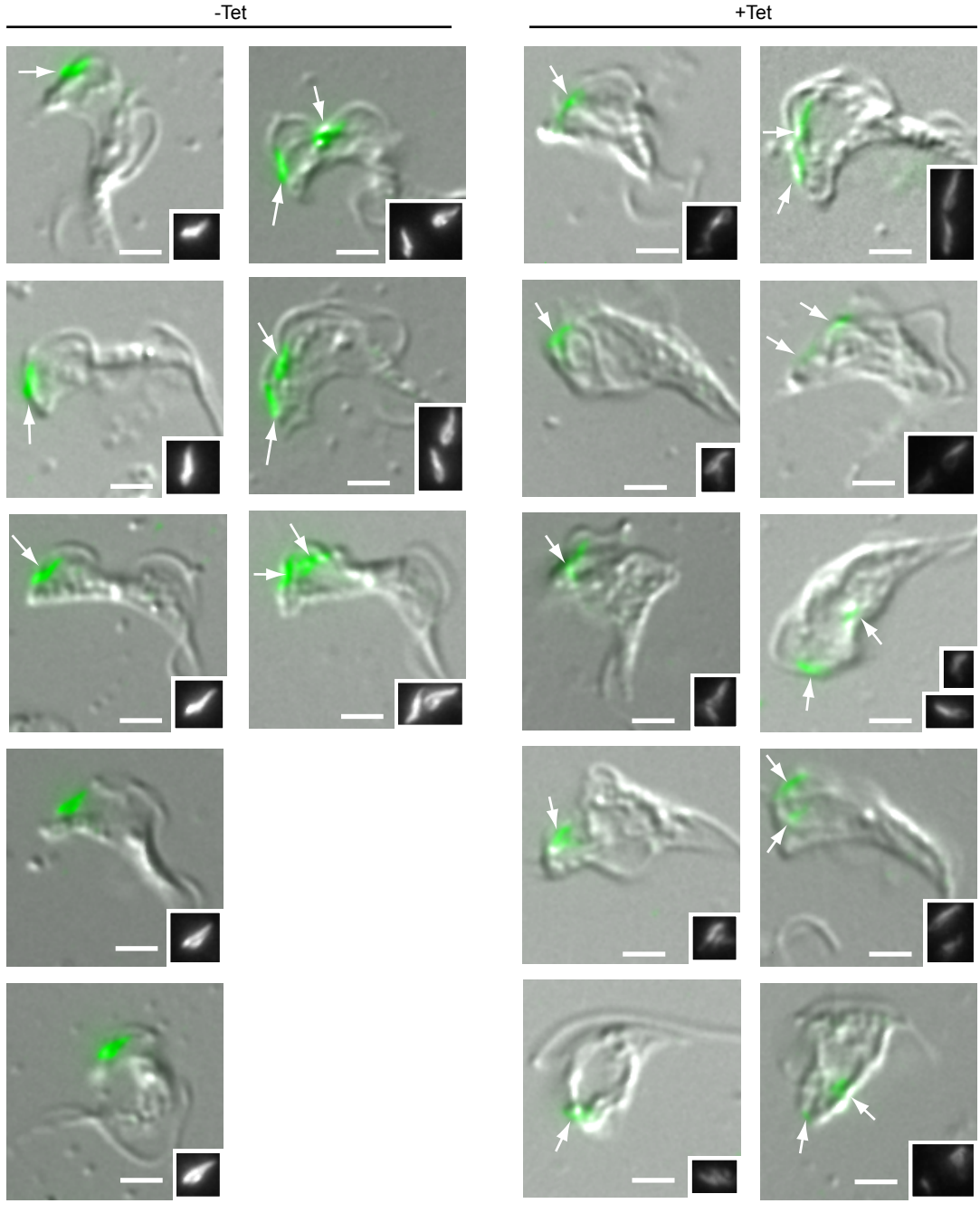

FIG. S2. TbMORN1 in control and induced cells. TbMORN1 RNAi cells from uninduced (- Tet) and induced (+ Tet, 14 h timepoint) populations were extracted with detergent, fixed, and labeled with anti-TbMORN1 antibodies. Immunofluorescence images were acquired using identical exposure times and are shown superimposed on differential interference contrast (DIC) images. Greyscale insets reproduce the structures indicated by arrows. The left-hand set of column in each category shows cells with a single TbMORN1 complex; the second column shows cells with two resolvable TbMORN1 complexes. Scale bars, 2 μm. Images are representative of >3 independent experiments.

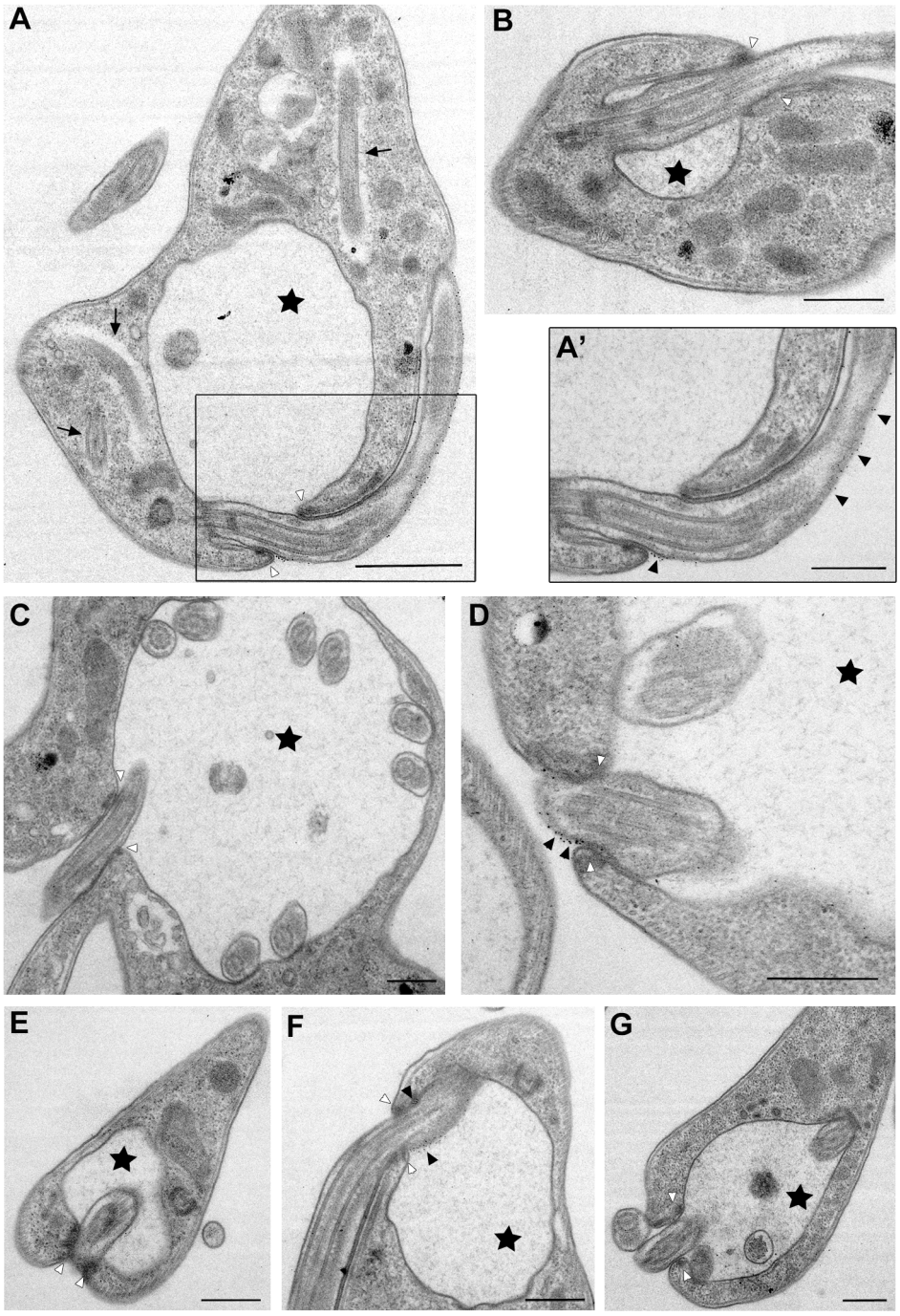

FIG. S3. Further examples of impaired BSA-5 nm gold uptake following TbMORN1 depletion. (A – G) TEM images taken from 60 nm thick resin sections contrasted with uranyl acetate and lead citrate of TbMORN1-depleted cells (14 h timepoint) after incubation with BSA-5 nm gold. FPs are indicated with stars; intracellular axonemes are indicated with arrows; the FPN is indicated with white arrowheads; gold particles near the FPN are indicated with black arrowheads. The FPN is always tightly associated with the exiting flagellum in TbMORN1-depleted cells, regardless of the extent of enlargement of the FP. Gold particles are mostly visible outside the FP. (A') is an enlargement of the boxed area in (A). Scale bars: A, 1 μm; A' to G, 500 nm.

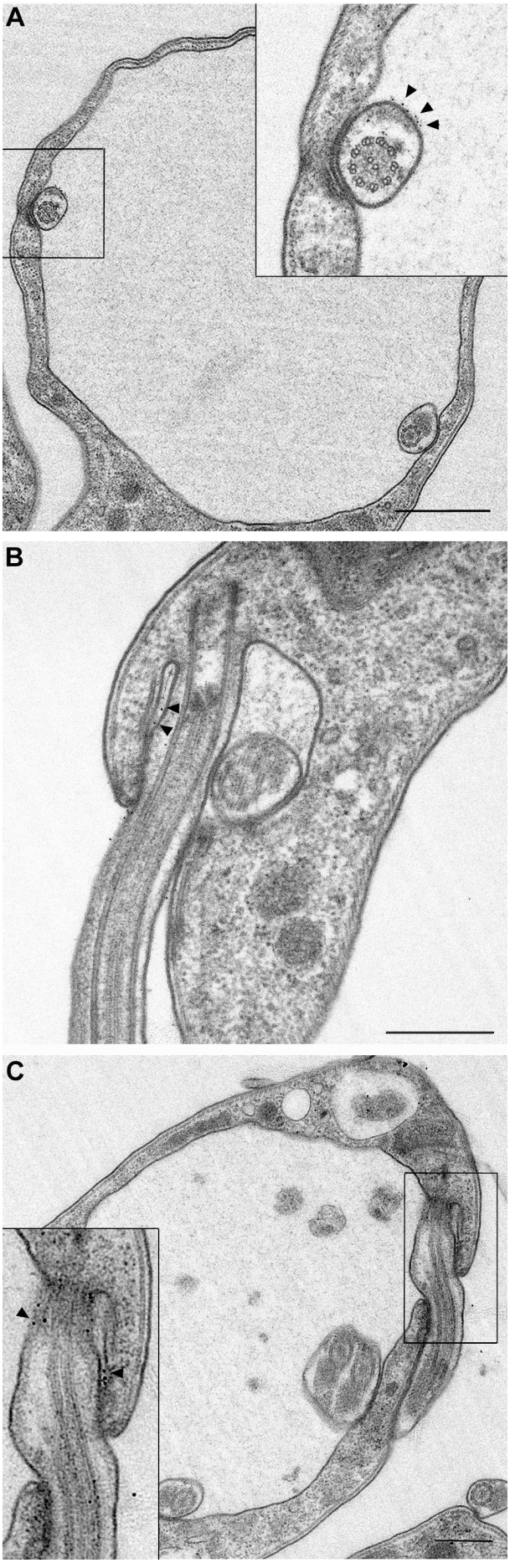

FIG. S4. BSA-gold can pass the flagellar neck in TbMORN1-depleted cells. (A – C) Images taken from 60 nm thick resin sections contrasted with uranyl acetate and lead citrate of TbMORN1-depleted cells (14 h timepoint) after incubation with BSA-5 nm gold. Arrowheads point at black particles of BSA-gold that have either passed the point of entry or are within the FPN. The insets in A and C are enlargements of the boxed areas. Scale bars: A, 1 μm; B, C, 500 nm.

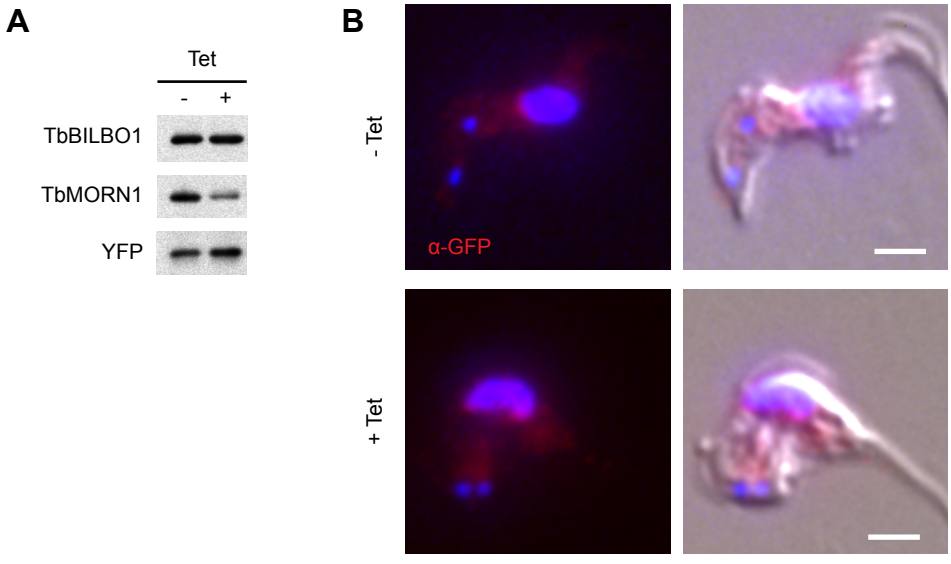

FIG. S5 Depletion of TbMORN1 does not appear to affect ss-YFP. (A) Immunoblots of whole-cell lysates taken from uninduced (- Tet) and induced (+ Tet) TbMORN1 RNAi cells expressing ss-YFP. Blotting with anti-TbBILBO1 antibodies confirmed that the samples were at the same concentration. Blotting with anti-TbMORN1 antibodies confirmed depletion. Blotting with anti-GFP antibodies (1) showed that there was not a gross change in the levels of ss-YFP. (B) Immunofluorescence analysis of TbMORN1 RNAi cells expressing ss-YFP (14 h timepoint). The YFP signal alone was too weak for detection, so anti-GFP antibodies were used. There was no gross change in the anti-GFP signal in TbMORN1-depleted cells. Scale bars, 2 μm. Data shown in this figure are representative of four inductions using two independent clones.

References:

1. **Seedorf, M., M. Damelin, J. Kahana, T. Taura, and P.A. Silver**. 1999. Interactions between a nuclear transporter and a subset of nuclear pore complex proteins depend on Ran GTPase. Mol. Cell. Biol. **19**:1547-1557.